THE ASTRONOMICAL JOURNAL, 115:1653–1663, 1998 April

RESONANCES IN THE EARLY EVOLUTION OF THE EARTH-MOON SYSTEM

JIHAD TOUMA
McDonald Observatory, University of Texas, Austin, TX 78712; touma@harlan.as.utexas.edu
AND
JACK WISDOM
Department of Earth, Atmospheric, and Planetary Sciences, Massachusetts Institute of Technology, Cambridge, MA 02139; wisdom@mit.edu
Received 1997 November 25; revised 1997 December 26

ABSTRACT

Most scenarios for the formation of the Moon place the Moon near Earth in low-eccentricity orbit in the equatorial plane of Earth. We examine the dynamical evolution of the Earth-Moon system from such initial configurations. We find that during the early evolution of the system, strong orbital resonances are encountered. Passage through these resonances can excite large lunar orbital eccentricity and modify the inclination of the Moon to the equator. Scenarios that resolve the mutual inclination problem are presented. A period of large lunar eccentricity would result in substantial tidal heating in the early Moon, providing a heat source for the lunar magma ocean. The resonance may also play a role in the formation of the Moon.

Key words: celestial mechanics, stellar dynamics — Earth — Moon

1. INTRODUCTION

The origin of the Moon is still unclear. The classic scenarios for the formation of the Moon include coaccretion, fission, and capture. Recent attention has focused on the giant-impact hypothesis, wherein a Mars-sized body has a grazing impact with a differentiated Earth and the resulting ejecta reaccrete to form the Moon. In all scenarios for the formation of the Moon except capture, the Moon accretes in a near-Earth orbit, which in turn suggests that the lunar orbit is initially in the equatorial plane with low orbital eccentricity. However, studies of the dynamical history of the Earth-Moon system have found that the Moon's orbit was highly inclined to Earth's equator when the Moon was close to Earth (see reviews by Burns 1986; Boss & Peale 1986). The existing dynamical histories are only consistent with the capture hypothesis. So either the dynamical histories are wrong or all of the scenarios that place the Moon initially in the equatorial plane are wrong. There are many proposed resolutions of this problem. Perhaps the tidal models are invalid at close distances. Or perhaps a second large impact on Earth or the Moon modified the inclination of the lunar orbit to the equatorial plane. Here we pursue a different line of investigation. Perhaps the orbital mechanics is richer than previously suspected. We have undertaken new studies of the evolution of the Earth-Moon system, with conventional tidal models, to examine this possibility.

In Touma & Wisdom (1994) we reexamined the evolution of the Earth-Moon system, recasting the model of Goldreich (1966) in Hamiltonian form. We confirmed the results of Goldreich, particularly his finding that the evolution of the system was strongly affected by cross-tidal interactions. We also confirmed his result that the qualitative behavior of the system is not strongly affected by the assumed frequency dependence of the tidal friction. The Goldreich model (and our Hamiltonian reformulation of it) is a multiply averaged secular model. In it, planetary perturbations are ignored. Earth's orbit is assumed to be circular, and the lunar orbit is also presumed to be circular. The equations of motion are averaged over the orbital periods of Earth and the Moon and averaged over the period of the regression of the Moon's node. With so many approximations, we thought it worthwhile to verify the evolution of the system with numerical simulation. Our hope was that through direct numerical simulation we would uncover something missed by the multiply averaged models. Our model integrates the motion of the Moon, all of the planets, and the Sun. It includes the rigid-body dynamics of Earth. We take into account second-order harmonics of Earth's gravitational field. We include an approximation for the relativistic precession of the planetary orbits. We use the constant time lag model of tidal friction from Mignard (1981). In our initial study, we enhanced the tidal friction to reduce the computational demands. To our chagrin, we found that the accelerated evolution was in excellent agreement with the predictions of the secular theory computed by Goldreich some 30 years earlier. However, the accelerated evolutions were undertaken with foreknowledge that, by accelerating the evolution, some resonance effects might be missed. We have subsequently carried out additional simulations with more realistic rates of tidal evolution and have now found that the system does indeed pass through strong resonances that can have a dramatic effect on the history of the Earth-Moon system. The fact that strong resonances are encountered necessitates a different approach to the study of the history of the Earth-Moon system, because passage through resonance is not time-reversible: capture into a resonance may be possible if the resonance is encountered from one direction but not from the other direction. Rather than starting at the present and working backward, we must now start with various presumed initial configurations and study the forward evolution. We have found that the dynamical evolution of the Earth-Moon system is much more complicated than the secular theories lead one to believe.

The first strong resonance that is encountered by the system occurs when the period of precession of the pericenter of the Moon is near 1 year. This resonance is known as the "evection." That the Earth-Moon system may have passed through the evection was pointed out by Kaula & Yoder (1976), but the importance of the evection resonance was discounted because attention was then focused on coaccretion formation scenarios that placed the Moon initially outside the resonance. We investigate the probability of capture into the evection resonance as a function of the rate of tidal evolution and the initial eccentricity. We derive analytic expressions for the track of the system in resonance, and we explore the mechanism of escape from the evection resonance. If dissipation in the Moon is neglected, the lunar eccentricity after escape from the evection is near 0.5; if dissipation in the Moon is taken into account the postevection eccentricity is less, but still substantial.

Following escape from the evection, the system passes through an inclination-eccentricity resonance, which we christen the "eviction." Passage through the eviction resonance is in the wrong direction for capture to occur but results in an excitation of the mutual inclination (the inclination of the lunar orbit to the equator) of about 2°–3°. We derive an analytic expression for the amplitude of this excitation.

Consequences of the passages of the Earth-Moon system through these resonances on the thermal evolution of the Moon are discussed. The very large values to which the eccentricity of the lunar orbit is excited imply significant tidal heating in the early Moon, enough to induce substantial melting.

If there is significant melting in the Moon, then the effective rigidity of the Moon may be reduced, resulting in an enhanced rate of energy dissipation (Peale, Cassen, & Reynolds 1979). We consider evolutionary scenarios with enhanced lunar dissipation after the initial passage through the evection and eviction resonances. Enhanced lunar dissipation causes the lunar eccentricity to decay but also results in an initial regression of the semimajor axis, allowing a second encounter with the eviction resonance. For this encounter, capture is almost certain provided that the rate of tidal evolution is small enough. After capture, evolution in the eviction resonance excites the mutual inclination to values as large as 12°. Subsequent evolution of the system can take the system to the present state of the Earth-Moon system. This scenario thus provides a possible resolution of the mutual inclination problem within conventional tidal models.

2. EVECTION AND EVICTION: BASIC PHENOMENOLOGY

We first show some results from a sample evolution of the Earth-Moon system through the evection and eviction resonances. In this simulation, we used the full numerical model as described in Touma & Wisdom (1994). We placed the Moon initially in the equatorial plane, with an initial eccentricity of 0.01 and a semimajor axis of $3.5R_E$, where R_E is the radius of Earth. The initial obliquity of Earth was 10°. The initial rotation period of Earth was 5.0 hr. The initial rate of the semimajor-axis evolution was set at 1 km yr^{-1}.

The eccentricity e of the lunar orbit as a function of the semimajor axis a of the Moon is shown in Figure 1. The system is captured into the evection resonance at about 4.6 R_E, and while captured in the resonance, the eccentricity of the Moon skyrockets to values above 0.5. At this point the system escapes from resonance. In the postevection evolution the eccentricity continues to increase.

In Figure 2, we show the mutual inclination ϵ of the lunar orbit to Earth's equator versus the semimajor axis a of the Moon. There are a number of distinctive features. The dominant feature is an excitation of the mutual inclination to about 2°.5 near $a = 6R_E$. This excitation occurred as the system passed through a resonance between the argument of the evection resonance and the node of the lunar orbit on Earth's equator. We call this resonance the "eviction."

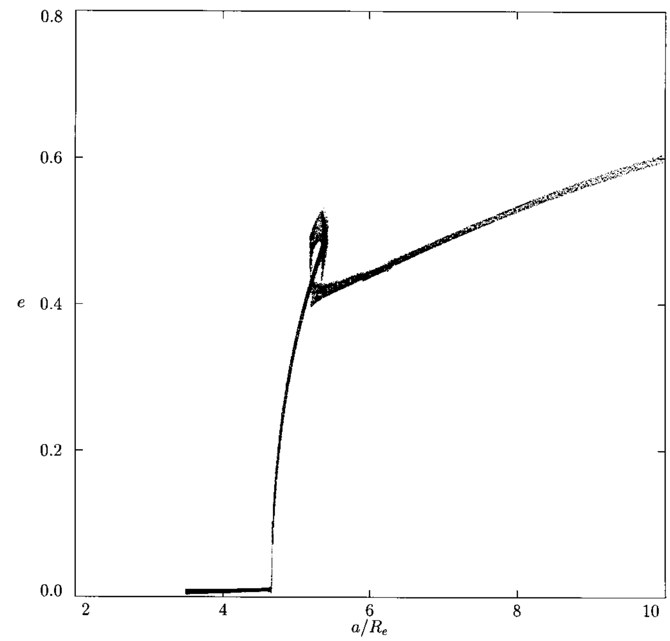

FIG. 1.—Plot of eccentricity vs. semimajor axis of the lunar orbit, illustrating the very strong effect the evection resonance may have on the evolution of the lunar orbit.

3. MODEL HAMILTONIAN

In this section we develop a simplified model Hamilto-

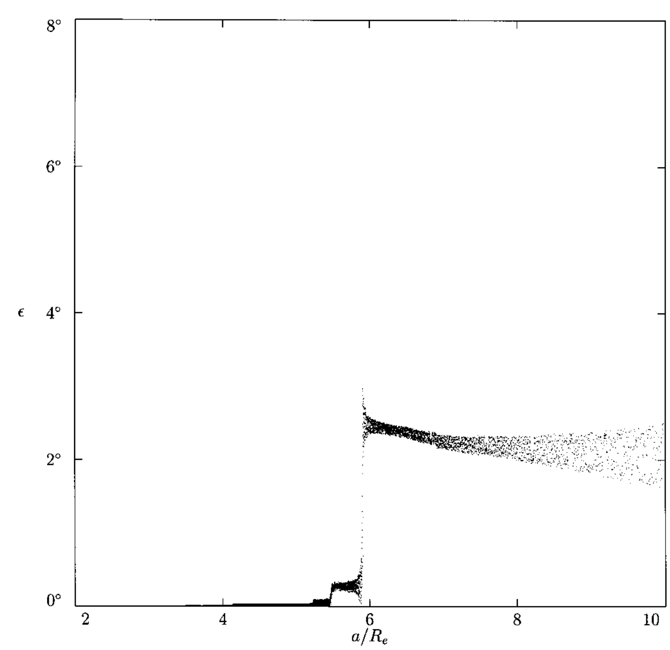

FIG. 2.—Plot of the Moon's inclination to Earth's equator vs. the semimajor axis of the lunar orbit, showing the Moon's eviction from the equator at about $6R_E$.

nian for the evection and eviction resonances, to better understand the full simulation results. For this model, we take Earth's orbit about the Sun to be fixed and circular and Earth's spin axis to be fixed in space with constant obliquity I and fixed longitude of the ascending node of the equator Ω_e.

We start with the Hamiltonian describing motion of the Earth-Moon system as given in Touma & Wisdom (1994, eq. [29]), omitting terms that have no direct effect on the lunar orbit:

$$H = -\frac{m_1' \mu^2}{2L_1^2} + \frac{Gm_0 m_1}{r_1'} \frac{J_2 R_E^2}{(r_1')^2} P_2(\cos\theta_1') - \frac{Gm_1 m_2}{r_2'} \frac{m_0}{\eta_1} \frac{(r_1')^2}{(r_2')^2} P_2\left(\frac{x_1' \cdot x_2'}{r_1' r_2'}\right) . \quad (1)$$

The first term represents the gravitational interaction of the Earth-Moon pair, the second term represents the effect of Earth's oblateness, and the last term is the leading term in the interaction of the Moon and the Sun. Jacobi coordinates are used in the development of the Hamiltonian. Here x_1' and x_2' are the Jacobi vector positions of the Moon and Sun, and r_1' and r_2' are the magnitudes of these vectors. The masses of Earth, the Moon, and the Sun are m_0, m_1, and m_2, respectively, and the Jacobi masses m_i' are given by $m_i' = m_i \eta_{i-1}/\eta_i$, with $\eta_i = \sum_{j=0}^{i} m_j$. We also have $\mu = Gm_0 m_1$. The Delaunay momentum conjugate to the mean anomaly l_1 of the lunar orbit is $L_1 = (m_1 \mu a_1)^{1/2}$, where a_1 is the semimajor axis of the lunar orbit. The Delaunay momentum $G_1 = L_1(1 - e_1^2)^{1/2}$ is conjugate to the argument of pericenter $g_1 = \omega_1$, where e_1 is the eccentricity of the lunar orbit, and the Delaunay momentum $H_1 = G_1 \cos i_1$ is conjugate to the longitude of the ascending node $h_1 = \Omega_1$, where i_1 is the inclination of the lunar orbit. The dimensionless second moment of Earth's gravitational field is J_2, and R_E is the radius of Earth. The angle between the symmetry axis of Earth and the vector from Earth to the Moon is denoted by θ_1'. We have omitted terms that govern the rotation of Earth, and the potential interaction of Earth and the Sun.

We develop the Hamiltonian in an equatorial reference frame. For this analysis the orbit of the Earth-Moon barycenter about the Sun is taken to be circular, with semimajor axis a_2 and mean motion n_2. In an equatorial reference frame, with the ascending node of the equator on the Earth-Sun orbital plane as the reference longitude, the components of the vector x_2' to the Sun are $[\cos(n_2 t - \Omega_e)$, $\cos I \sin(n_2 t - \Omega_e)$, $-\sin I \sin(n_2 t - \Omega_e)]$. The vector x_1' from Earth to the Moon has components $R_z(\Omega) R_x(i) R_z(\omega) \times (r_1 \cos\theta, r_1 \sin\theta, 0)$, where r_1 is the distance from Earth to the Moon, θ is the true anomaly, ω is the argument of pericenter, ϵ is the inclination of the lunar orbit to the equator, and Ω is the ascending node of the lunar orbit relative to the equinox. The functions R_x and R_z generate active right-hand rotations about the named axis. The detailed development of the terms in the Hamiltonian is straightforward. Expressing the Hamiltonian as a Poisson series, we can pick out those terms that correspond to the resonances of interest. The resonance Hamiltonian is

$$\begin{aligned} H_{\rm res} = &-\frac{m_1' \mu^2}{2L_1^2} + \frac{Gm_0 m_1}{r_1'} \frac{J_2 R_E^2}{(r_1')^2} \\ &\times \left\{\frac{3}{4}\sin^2\epsilon[1 - \cos 2(\theta + \omega)] - \frac{1}{2}\right\} \\ &- \frac{Gm_1 m_2}{a_2} \frac{m_0}{\eta_1} \frac{(r_1')^2}{a_2^2} \\ &\times \left\{\frac{3}{4}\cos^4\frac{\epsilon}{2}\cos^4\frac{I}{2}\cos 2(n_2 t - \Omega_e - \theta - \omega - \Omega)\right. \\ &-\frac{3}{4}\cos^2\frac{\epsilon}{2}\cos^2\frac{I}{2}\sin\epsilon\sin I \\ &\left.\times \cos[2(n_2 t - \Omega_e - \theta - \omega - \Omega) + \Omega]\right\} . \end{aligned} \quad (2)$$

There are other resonance terms that are higher order in mutual inclination and obliquity that may be important for slower rates of tidal evolution. Averaging over the lunar orbital period and making a canonical transformation to the resonance variable $\sigma = n_2 t - \Omega_e - \omega - \Omega$ with the generating function

$$F_2 = (l_1 + g_1 + h_1)L' + (n_2 t - \Omega_e - g_1 - h_1)\Sigma - h_1 \Psi \quad (3)$$

yields

$$\begin{aligned} \bar{H}_{\rm res}' = &\, n_2 \Sigma + n_1 J_2 \left(\frac{R_E}{a_1}\right)^2 L' \left(\frac{3}{4}\sin^2\epsilon - \frac{1}{2}\right) \frac{1}{(1 - e^2)^{3/2}} \\ &- \frac{15}{8} e^2 n_2 \frac{n_2}{n_1} L' \cos^4\frac{\epsilon}{2}\cos^4\frac{I}{2}\cos 2\sigma \\ &+ \frac{15}{8} e^2 n_2 \frac{n_2}{n_1} L' \cos^2\frac{\epsilon}{2}\cos^2\frac{I}{2}\sin\epsilon \\ &\times \sin I \cos(2\sigma - \psi) . \end{aligned} \quad (4)$$

We have dropped the constant term that controls the mean longitude. The mean longitude $\lambda = l_1 + g_1 + h_1$ is conjugate to the momentum $L' = L_1$. The resonance angle σ is the difference of the longitude of the Sun and the longitude of the pericenter. The momentum $\Sigma = L_1 - G_1$ is conjugate to the resonance angle σ; the momentum $\Psi = G_1 - H_1$ is conjugate to $\psi = -h_1 = -\Omega$. Note that

$$e^2 = \frac{\Sigma}{L'}\left(2 - \frac{\Sigma}{L'}\right) \quad (5)$$

and that

$$\sin^2\frac{\epsilon}{2} = \frac{\Psi}{2(L' - \Sigma)} . \quad (6)$$

The evection resonance is associated with the term with argument 2σ, and the eviction resonance is associated with the term with argument $2\sigma - \psi$. The largest periodic variations in the longitude of the Moon are known as the "evection" and can be traced to the 2σ term in the Hamiltonian (see Brouwer & Clemence 1961). These variations were known to Hipparchus. With others (e.g., Kaula & Yoder 1979), we adopt "evection" as the name of the resonance arising from this same term. The term associated with the eviction resonance is closely related to the evection resonance term but has a stronger effect on the inclination of the

Moon's orbit than on the eccentricity. Our name for this resonance is "eviction"—that is, "evection" with an *i* rather than an *e*. It is the resonance that *evicts* the Moon from the equatorial plane.

4. A SIMPLE MODEL OF EVECTION

A simple model of the evection is obtained by neglecting the eviction resonance and ignoring the small mutual inclination and obliquity. The approximate evection Hamiltonian is then

$$H_e = n_2 \Sigma - \frac{1}{2} n_1 J_2 \left(\frac{R_{\mathrm{E}}}{a_1}\right)^2 L' \frac{1}{(1-e^2)^{3/2}} - \frac{n_2^2}{n_1} L' e^2 \frac{15}{8} \cos 2\sigma \,. \tag{7}$$

The eccentricity becomes quite large, but it is instructive to study the evection resonance Hamiltonian under the additional assumption of small eccentricity. Keeping nonresonant terms up to order Σ^2 and resonant terms to order Σ, we find

$$H_e \approx \left(n_2 - \frac{3}{2} J_2 \frac{R_{\mathrm{E}}^2}{a_1^2} n_1\right)\Sigma - 3n_1 J_2 \frac{R_{\mathrm{E}}^2}{a_1^2} \frac{1}{L'} \Sigma^2 - \frac{n_2^2 15}{n_1 4} \Sigma \cos 2\sigma \,, \tag{8}$$

which is a familiar approximation for second-order resonances. The quantity in parentheses is the difference of the mean motion of the Sun and the rate of precession of the pericenter of the Moon due to the oblateness of Earth; this frequency combination provides a measure of the distance to resonance. The oblateness of Earth depends on its rotation rate: we assume $J_2 = J_{20}(\omega/\omega_0)^2$, where J_{20} is the value of J_2 for the rotation rate ω_0. The present value of J_2 is about $J_{20} = 0.001083$. For a rotation rate of 5.2 hr, we find $J_2 \approx 0.023$. Thus the resonance occurs near $a_1 \approx 4.64 R_{\mathrm{E}}$, which is indeed about where we find it. The evection resonance Hamiltonian has a single degree of freedom, so the trajectories are the same as the level curves of the Hamiltonian. In examining the level curves it is convenient to introduce rectangular coordinates via the canonical transformation $\xi = (2\Sigma)^{1/2} \cos \sigma$ and $\eta = (2\Sigma)^{1/2} \cos \sigma$, where ξ is the momentum conjugate to η. The truncated evection Hamiltonian is

$$H_e \approx \delta\left(\frac{\xi^2+\eta^2}{2}\right) - \alpha\left(\frac{\xi^2+\eta^2}{2}\right)^2 - \beta\left(\frac{\xi^2-\eta^2}{2}\right), \tag{9}$$

with

$$\delta = n_2 - \frac{3}{2} J_2 \frac{R_{\mathrm{E}}^2}{a_1^2} n_1 \,, \tag{10}$$

$$\alpha = 3n_1 J_2 \frac{R_{\mathrm{E}}^2}{a_1^2} \frac{1}{L'} \,, \tag{11}$$

$$\beta = \frac{n_2^2}{n_1} \frac{15}{4} \,. \tag{12}$$

The fixed points have either $\xi = 0$ or $\eta = 0$. For $\xi = 0$, the fixed points have $\eta = 0$ or $\eta = [(\delta + \beta)/\alpha]^{1/2}$. For $\eta = 0$, the fixed points have $\xi = 0$ or $\xi = [(\delta - \beta)/\alpha]^{1/2}$. The fixed point at the origin always exists. The fixed points away from the origin only exist if the quantity in the square root is positive. For $\delta \geq -\beta$ then there is a pair of symmetrically placed fixed points with $\xi = 0$. For $\delta \geq \beta$ there are, in addition, symmetrically placed fixed points with $\eta = 0$. The level curves show that the origin is an unstable fixed point for $-\beta < \delta < \beta$, the fixed points on the η-axis with $\xi = 0$ are stable, and the fixed points on the ξ-axis with $\eta = 0$ are unstable.

The eccentricity of the stable fixed point of the truncated averaged evection resonance Hamiltonian (eq. [9]) is compared with the eccentricity in the numerical evolution in Figure 3. Also shown is the eccentricity of the stable fixed point of the full averaged evection resonance Hamiltonian (eq. [7]). We see that the truncated model does quite well even at high eccentricity, though the full resonance model does better. In tracking the fixed points, we compute the constants δ, α, and β for each lunar semimajor axis a_1. Though the variation of δ has the strongest effect on the level curves and fixed points, including the variation of α and β with a_1 improves the agreement of the fixed points with the simulation. Evidently, as far as the evolution of the eccentricity through the evection resonance is concerned, the actual nonzero obliquity has little effect, as one would expect from the fact that the obliquity only enters through a factor of $\cos^4 (I/2)$.

4.1. *Probability of Capture into Evection*

Next we calculate the capture probability. If the passage through resonance is very slow (we call this the "adiabatic limit"), the calculation of capture probabilities is straightforward (Yoder 1979; Henrard 1982; Borderies & Goldreich 1984). In the adiabatic limit, if a second-order resonance is encountered with increasing δ (for positive α and β), then capture is certain if the eccentricity is smaller than a critical value. This is the case that applies for tidal evolution of the Moon away from Earth. We find that the critical eccentricity is 0.0773. That is, if the evolution is slow enough and the eccentricity is below 0.0773, then the system

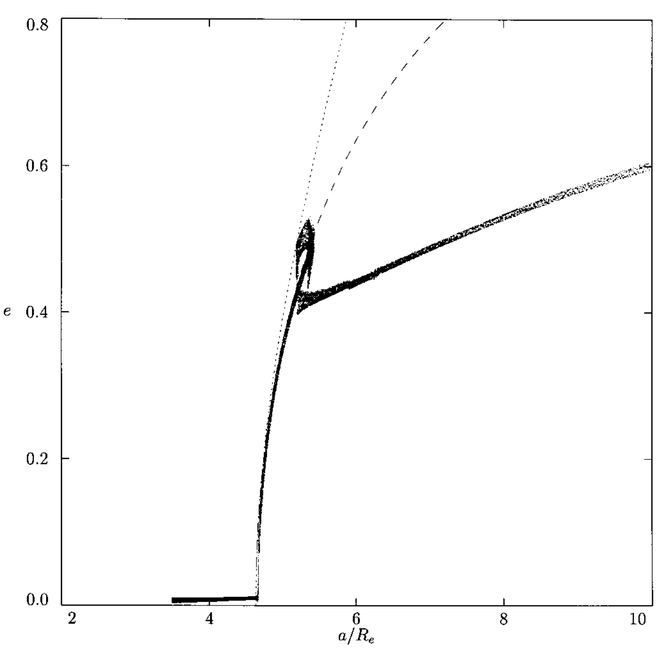

FIG. 3.—Stable fixed point of the truncated resonance model (*dotted line*) and of the full resonance model (*dashed line*) compared with the tidally evolving eccentricity in the full simulation.

is certainly captured into the evection resonance. If the resonance is encountered with larger eccentricity, the system may be captured or not, depending on the phases. With an initial random phase assumption, the probability of capture is the ratio of the rate of increase of the area on the phase plane of the libration island to the rate of increase of the sum of the phase plane area of the libration island and the region on the phase plane corresponding to escape (inner circulation). For the truncated resonance Hamiltonian, there are analytic expressions for the capture probabilities (Borderies & Goldreich 1984). For the more accurate untruncated evection resonance Hamiltonian, we have to compute the appropriate integrals numerically. The calculations are straightforward, so we will not show the details. The results are displayed in Figure 4. Again, the truncated resonance model agrees rather well with the full evection resonance model.

4.2. *Nonadiabatic Capture Probability*

Unfortunately, it is not clear whether the adiabatic capture probabilities apply or not, because the rate of tidal evolution of the lunar orbit when the Earth-Moon separation is small is uncertain. We can anticipate that in the limit that the evolution is very rapid, the resonance will have little effect and capture will not occur. If the evolution is very slow, the adiabatic estimates will apply. For intermediate rates of evolution the situation is more complicated. The transition region can be identified by carrying out numerical experiments for varying rates of tidal evolution and comparing the observed capture probabilities with the adiabatic capture probabilities. We investigated $da/dt = 1$ km yr^{-1} and $da/dt = 10$ km yr^{-1}. It turns out that these rates approximately bracket the transition from adiabatic transition to nonadiabatic transition of the evection resonance. Capture probabilities were estimated by running 100 simulations with the initial angle of the argument of pericenter distributed uniformly. The results are displayed in Figure 4. The error estimates are $\sigma = [p(1-p)/N]^{1/2}$, where p is the fraction captured and N is the number of trials. We see that the capture probabilities for a tidal evolution rate of 1 km yr^{-1} are close to those predicted by the adiabatic theory. Note that at small eccentricity, capture is not certain even for this rate of evolution. For a faster evolution of 10 km yr^{-1}, the capture probabilities at small eccentricity are significantly smaller.

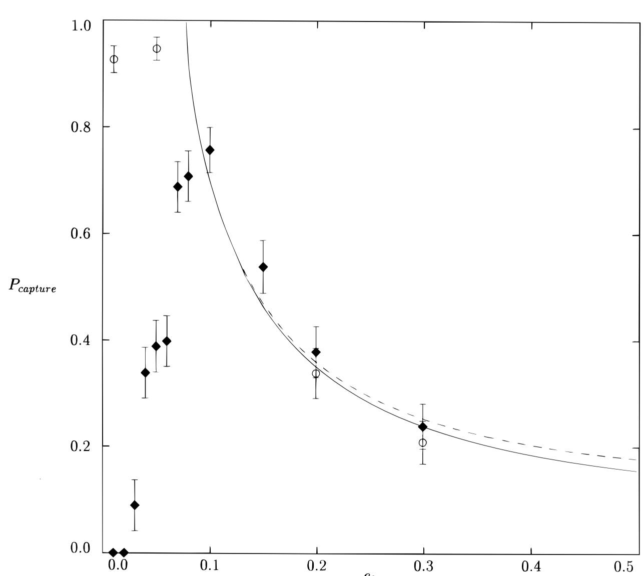

FIG. 4.—Capture probability for the evection resonance as a function of the eccentricity well before resonance encounter. The solid line is for the full evection resonance Hamiltonian, and the dashed line is for the truncated evection resonance Hamiltonian. Plotted with the adiabatic capture probabilities are the results of some numerical experiments. The circles show the capture probabilities determined with a tidal evolution rate of 1 km yr^{-1}; the diamonds show the capture probabilities for an evolution rate of 10 km yr^{-1}.

The Mignard model with constant time lag that we have used for our simulations predicts a rate of evolution of the semimajor axis at the evection of about 150 km yr^{-1}. Of course, this rate is suspect for many reasons. It is unlikely that this simple model accurately models the tidal interactions at such small distances, but even within the context of model evolutions constructed with the Mignard tide, we do not know how the tidal effective Q of Earth and the Moon have varied with time. Lunar histories based on either frequency-dependent or frequency-independent Darwin tides place the Moon close to Earth less than 2×10^9 years ago, yet the Moon does not show any evidence of such a recent encounter. In order to solve this timescale problem, the effective Q of Earth must either have been larger in the past or the system must have encountered some dynamically interesting region that slowed the overall evolution. Given that we do not know of any dynamical mechanism to restrain the evolution of the lunar orbit, we must assume the effective Q has changed. Indeed, there is reason to believe that the Q of Earth was larger in the past, because the current Q is largely due to dissipation in the oceans and the ocean response may be resonantly enhanced. We can place a lower limit on the average early Q in the following way: There is evidence (e.g., Sonnet et al. 1996) that the current rate of tidal evolution was typical for the last 10^9 years. At this point the Earth-Moon separation is near $50R_{\rm E}$. If at this point the Earth Q is enhanced so that the Moon is close to Earth 4.6×10^9 years ago, then we find that the Q must be enhanced by a factor of about 25. If the enhancement occurred earlier, then it would have to be appropriately larger. With an enhancement factor of 25, the Mignard model would yield a rate of tidal evolution at the evection of about 6 km yr^{-1}. For the constant phase lag models, the deduced rate of evolution at the evection is smaller, about 4 km yr^{-1}. Of course these rates should not be taken too seriously. For most of its history the Moon is far from Earth (assuming constant time lag, the Moon has been outside $40R_{\rm E}$ for 95% of the time since formation), so the average rate of evolution does not really constrain the rate of evolution during the earlier phase. In any case, the deduced rate of evolution is right in the middle of the region that bounds the transition from adiabatic to nonadiabatic capture probabilities. The situation could hardly be worse for determining a unique history of the Earth-Moon system. Consequently, we must consider histories both with and without capture at the evection resonance.

5. NONCAPTURE PASSAGE THROUGH EVECTION

For adiabatic rates of evolution, if the evection resonance is encountered with an eccentricity above the critical eccentricity and the system is not captured, then the eccentricity after resonance passage is lower than the initial eccentricity. Here we are focusing on the situation in which the initial

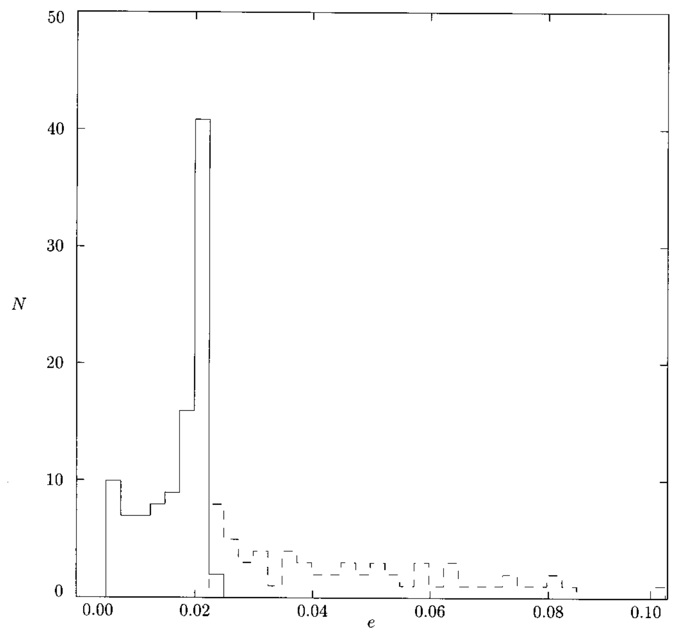

FIG. 5.—Distribution of eccentricity after evection for $e = 0.01$ (*solid histogram*) and $e = 0.05$ (*dashed histogram*) before encounter. At these eccentricities, capture should occur if the evolution is slow enough; passage through the resonance occurs for faster evolution. The postevection eccentricity is not predicted by the adiabatic theory. In these numerical experiments a postevection eccentricity near 0.02 occurs frequently, but there is a large spread.

eccentricity is below the critical eccentricity and escape occurs because the evolution is nonadiabatic. The adiabatic picture no longer predicts the postevection eccentricity. In simulated evolutions through the evection resonance with 10 km yr^{-1} semimajor-axis evolution rate, the capture probability is low at low eccentricities (see Fig. 4). The

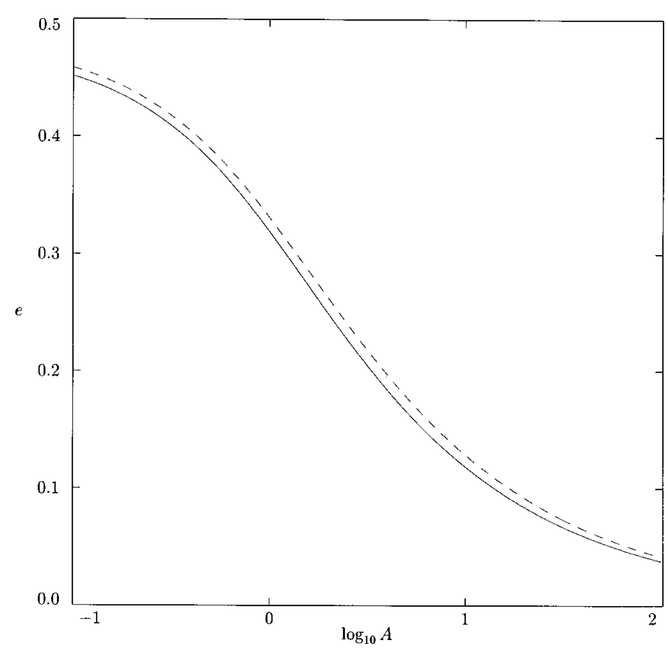

FIG. 6.—Eccentricity for which the semimajor axis is at an equilibrium with respect to tidal evolution vs. the logarithm of the A-parameter, which is a measure of the relative dissipation in the Moon and Earth. This eccentricity approximates the eccentricity of the lunar orbit after the system escapes from the evection resonance. The dashed curve includes only the direct effect of tides on the semimajor axis. The solid curve includes the additional small indirect effect of the tides on the eccentricity.

eccentricity is modified by the resonance passage; Figure 5 shows a histogram of the eccentricity after evection for those experiments in which the evection resonance did not capture the system. Small initial eccentricities are typically increased; initial eccentricities closer to the critical eccentricity are typically decreased. It looks as though there is a clustering of eccentricity at about 0.02 in these experiments, but there is a wide spread. After a nonadiabatic passage through the evection resonance, the system does not have a characteristic eccentricity. This is unfortunate because the subsequent evolution of the eccentricity depends sensitively on the initial eccentricity. The rate of growth of eccentricity is proportional to eccentricity, so the initial seed for the eccentricity dramatically affects the subsequent evolution. Even with dissipation in the Moon many of these evolutionary tracks develop large eccentricity, which can only be damped by enhanced tidal dissipation during some phase of the subsequent evolution. Some aspects of this evolutionary branch are discussed below.

6. CAPTURE AND ESCAPE FROM THE EVECTION RESONANCE

If the system is captured by the evection resonance, then the eccentricity of the lunar orbit grows rapidly. The system tracks the stable fixed point of the Hamiltonian model. At an eccentricity near 0.5 the system escapes from the resonance. The mechanism of escape is as follows: As the eccentricity increases, an eccentricity is reached for which the rate of tidal evolution of the semimajor axis vanishes. The approximate value of the eccentricity at which the semimajor axis ceases to evolve is the eccentricity at which the angular motion of the Moon at pericenter is faster than the angular rate of rotation of Earth. At this point, the eccentricity continues to evolve and the amplitude of the libration increases until the system leaves the resonance. There is no tidal equilibrium as there is for the Galilean satellites. For Io, the equilibrium eccentricity is also determined by the condition that the rate of evolution of the semimajor axis must vanish, but in that case the libration amplitude is decreased by the subsequent tidal evolution. Here the resonance is unstable to further tidal evolution, so capture in the evection resonance is always temporary.

Interestingly, escape from the evection can occur to either side of the resonance. If escape occurs to smaller semimajor axis, the semimajor axis regresses momentarily as the eccentricity decreases. Then the semimajor axis resumes its outward evolution. The evection resonance is then encountered again at high eccentricity. This time there is much smaller probability of capture (see Fig. 4), and the system typically passes through the evection with a decrease in eccentricity. Alternatively, the system may escape the evection resonance to the larger semimajor axis side of the resonance, and the semimajor axis continues to evolve outward from there.

The eccentricity at which the system escapes the evection resonance depends on how much energy dissipation there is in the Moon. It is known that dissipation in the Moon can strongly affect the orbital eccentricity of natural satellites (Goldreich 1963). We used the average Mignard (1981) tides for zero lunar obliquity to model the effect of tidal dissipation in the Moon on the lunar orbit. In these, the parameter

$$A = \frac{k_2'}{k_2}\frac{\Delta t'}{\Delta t}\left(\frac{m_0}{m_1}\right)^2\left(\frac{R_M}{R_E}\right)^3 \tag{13}$$

is a measure of the relative rates of energy dissipation in Earth and the Moon. Here k_2 and k_2' are respectively the potential Love numbers of Earth and the Moon, m_0 and m_1 are the masses of Earth and the Moon, Δt and $\Delta t'$ are the tidal time delay for Earth and the Moon, and R_E and R_M are the radii of Earth and the Moon. From lunar laser ranging results, the parameter A is estimated to be about 1.1 today (Dickey et al. 1994). Its value when the Earth-Moon system was near the evection resonance is unknown. In the derivation of the Mignard expressions it is assumed that the rotation of the Moon is locked in the synchronous state, which may not be correct.

With dissipation in the Moon, there is a critical value of the eccentricity for each semimajor axis above which the semimajor axis decreases rather than increases. In Figure 6, the value of eccentricity for which the tidal evolution of the semimajor axis halts is shown as a function of A. At the critical eccentricity, the rate of change of the semimajor axis is zero. This eccentricity approximates the eccentricity of the lunar orbit after the system escapes from the evection resonance. We include two contributions to the rate of change of the semimajor-axis evolution in the evection resonance. There is the direct average tidal contribution. In addition, there is a contribution from the tidal change in the eccentricity with the constraint between semimajor axis and eccentricity that the system remain at the resonance equilibrium. This latter effect is small.

7. TIDAL HEATING DURING EVECTION PASSAGE

The time evolution of the eccentricity during the evection resonance passage determines the extent of tidal heating in the Moon. The evolution of the eccentricity depends on the relative rates of tidal dissipation in Earth and the Moon. In Figure 7, the time evolution of the eccentricity of the lunar orbit is shown for $A = 0$, 1, 3, and 10. As the dissipation in the Moon increases, the peak eccentricity decreases. For these runs the semimajor axis evolves at 1 km yr^{-1}.

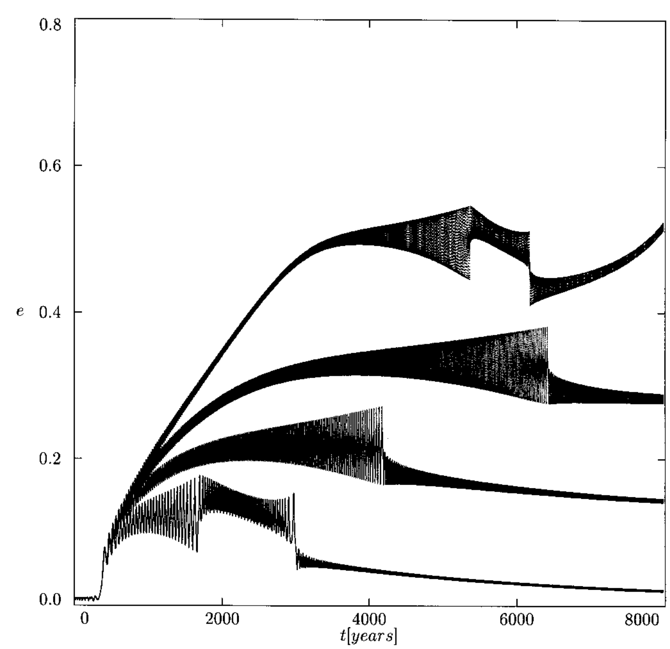

FIG. 7.—Eccentricity as a function of time for simulations with $A = 0$, 1, 3, and 10. As A increases, the peak eccentricity decreases.

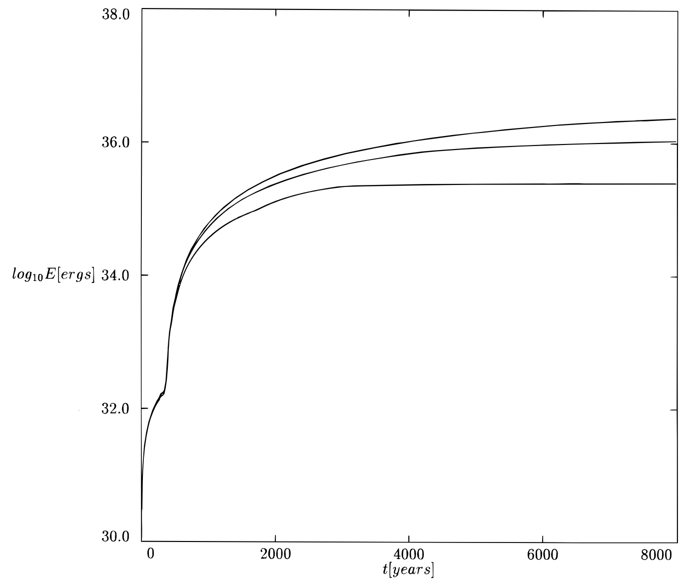

FIG. 8.—Accumulated total energy deposited in the Moon for $A = 1$, 3, and 10.

The Moon is strongly heated if the system is captured in the evection resonance. In Figure 8, the cumulative energy deposited is plotted versus time. These are the same runs for which the eccentricity is displayed in Figure 7. For the rate of energy deposition we use the expression of Yoder & Peale (1981),

$$\frac{dE}{dt} = \frac{42}{19}\frac{\pi e^2 \rho^2 R^7 n^5}{\mu Q}, \tag{14}$$

where e is the orbital eccentricity, ρ is the mean lunar density, R is the lunar radius, n is the mean motion, μ is the effective rigidity, and Q is the effective tidal Q for the Moon. There are too many uncertain parameters to unambiguously relate the rate of tidal evolution (as given by a Mignard time lag) and an A-parameter (which is a measure of relative dissipation in the Moon and Earth) to an effective Q for the Moon to be used in this formula. As a point of reference, we adopt, following Peale & Cassen (1978), $\mu = 6.5 \times 10^{11}$ dyn cm^{-1} and $Q = 100$. These values might be suitable for estimating tidal heating in an early Moon with a cool interior. It is likely that tidal heating would be greater than these values imply. For instance, the Q deduced from laser ranging is smaller than that used here, so if the laser-ranging value is more appropriate then we have underestimated the tidal heating. Also, if the Moon is strongly heated the rigidity is likely to decrease, perhaps substantially, further enhancing the rate of tidal heating above the simple estimate. We have neglected contributions due to nonzero obliquity of the Moon, and assumed synchronous rotation. Nonzero obliquity and nonsynchronous rotation would only increase the actual rate of tidal dissipation. Considering all these uncertainties, the actual tidal heating rate is difficult to predict, but the energy deposited in the Moon during this epoch is apparently of order 10^{36} ergs. Using a specific heat of 10^7 ergs g^{-1} K, we find the temperature of the Moon as a whole rises by more than 1000 K, surely sufficient to melt substantial portions of the Moon.

Strong tidal heating during evection passage provides an abundant energy source for the creation of the lunar magma ocean, and for interior heating that is later manifested in mare volcanism. However, an issue that must be addressed is whether such tidal heating can be ruled out on the basis of the radius constraint of Solomon & Chaiken (1976). They found that the observed paucity of extensional and compressional features on the Moon implies that the radius of the Moon has changed by less than ± 1 km since the end of the heavy bombardment, and that this could only be accomplished with a magma ocean if the interior of the Moon was initially cool. Essentially the same conclusions were drawn by Solomon & Longhi (1977), Cassen et al. (1979), Kirk & Stephenson (1989), and others, who have considered different aspects of the thermal evolution of the Moon. The difficulty is that tidal heating is strongest in the center of the Moon (Peale & Cassen 1978). So if tidal heating were responsible for the magma ocean, the interior would initially have been hot. Perhaps it is time to revisit the lunar thermal histories, with a possible passage through the evection resonance in mind.

8. ROLE OF EVECTION IN LUNAR FORMATION

Before leaving the evection, we mention an alternate role that the evection resonance may play in the history of the Earth-Moon system. A detailed picture of how the Moon reaccretes after the giant impact has not yet emerged. Even the timescale of reaccretion is uncertain by a couple orders of magnitude. For instance, in the *N*-body simulations of Ida, Canup, & Stewart (1997) the Moon quickly reaccretes, in a time of order 1 year or less. Thompson & Stevenson (1988) find that the reaccretion is much slower, on the order of several hundred years.

Without passing judgment on these investigations, we note that the evection resonance would certainly have an effect on the reaccretion of the Moon and the evolution of the protolunar disk. The evection is a very strong resonance and could play many different roles in the formation of the Moon. For instance, the evection could affect the evolution of the protolunar disk through resonance-disk interactions, or the evection could dramatically change the evolution of a swarm of moonlets. The simulations of Ida et al. (1997) suggest that a significant portion of the protolunar disk is lost to recollision with Earth and escapes from the system, and therefore that the impactor must be much larger than has been heretofore supposed. The evection could provide a holding point for runaway moonlets that are captured into the resonance, perhaps mitigating the problem of the runaway disk material. The evection resonance could even be the point of formation of the Moon. We mention though that there are two distinct phases for the evection equilibrium, and streamlines for these two phases cross. So material cannot simultaneously occupy both equilibria without collisions. There are many facets of the role of evection in lunar formation to be explored.

9. A SIMPLE MODEL OF EVICTION

If the system was captured by the evection resonance, then we expect that the lunar orbit had a large eccentricity upon escape from the resonance. If the eccentricity is large, the mixed eccentricity-inclination resonances can have a significant effect. We turn now to the analysis of the largest of these—the eviction. The eviction is associated with the last term in the average resonance Hamiltonian (eq. [4]). The eviction resonance acts in the postevection region to excite the mutual inclination. Here we develop a simple model of the eviction and use the model to develop approximate analytic estimates of the excitation of the mutual inclination.

For the analysis of the eviction resonance, we assume that the eccentricity is fixed, and the evection resonance is neglected. The approximate eviction Hamiltonian is then

$$H_i = n_2 \Sigma + n_1 J_2 \left(\frac{R_E}{a_1}\right)^2 L' \left(\frac{3}{4}\sin^2\epsilon - \frac{1}{2}\right) \frac{1}{(1-e^2)^{3/2}} + \frac{n_2^2}{n_1} L' e^2 \frac{15}{8} \cos^2\frac{I}{2} \sin I \cos^2\frac{\epsilon}{2} \sin\epsilon \cos(\psi - 2\sigma) . \tag{15}$$

We make a canonical transformation to the eviction resonance angle with the generating function

$$F_2 = (\psi - 2\sigma) R + \sigma S , \tag{16}$$

which yields $r = \psi - 2\sigma$ conjugate to $R = \Psi$ and $s = \sigma$ conjugate to $S = \Sigma + 2\Psi$. In the approximation that the evection resonance is far enough away in frequency for the eviction resonance to be considered separately, the momentum S is conserved. This appears to be the case for the evolution of the lunar orbit. The momentum $S \approx L'e^2/2$. We expand the eviction resonance Hamiltonian in powers of S/L' and powers of R/L'. We keep nonresonant terms to order R^2 and the lowest order resonant terms. The Hamiltonian is then in a standard form for a first-order resonance:

$$H_i = AR^2 + BR + C\sqrt{2R}\cos r , \tag{17}$$

with

$$A = -\frac{99}{4}\frac{n_1 J_2}{L'}\left(\frac{R_E}{a_1}\right)^2 \left[1 + 5\frac{S}{L'} + 15\left(\frac{S}{L'}\right)^2 + \cdots\right],$$

$$B = -2n_2 + \frac{9}{2} n_1 J_2 \left(\frac{R_E}{a_1}\right)^2 \left[1 + 4\frac{S}{L'} + 10\left(\frac{S}{L'}\right)^2 + 20\left(\frac{S}{L'}\right)^3 + \cdots\right],$$

$$C = \frac{15}{8} S \frac{1}{\sqrt{L'}} \frac{n_2^2}{n_1} \cos^2\frac{I}{2} \sin I . \tag{18}$$

The coefficient B is a measure of the distance from the resonance.

With the canonical change of variables $p = (2R)^{1/2}\cos r$ and $q = (2R)^{1/2}\sin r$, the Hamiltonian takes the form

$$H_i = A\left(\frac{p^2+q^2}{2}\right)^2 + B\left(\frac{p^2+q^2}{2}\right) + Cp . \tag{19}$$

The fixed points of the Hamiltonian occur on the $q = 0$ axis and satisfy $\partial H_i/\partial p = 0$. For negative A, there is a single stable fixed point for negative B. For large positive B there are three fixed points: two stable and one unstable. The bifurcation occurs at $B_c = -3(C^2 A/4)^{1/3}$, which is positive for negative A.

As the Moon evolves outward from the evection toward the eviction, the coefficient B is initially positive, and the area on the (p, q) eviction phase plane is small. When the system reaches the bifurcation point $B = B_c$, the fixed point that the system is near disappears (by collision with the unstable fixed point), and the system follows a new path encircling the sole remaining fixed point with finite area on the phase plane. The encounter of the resonance is in the wrong direction for capture, but mutual inclination of the lunar orbit is excited as the resonance is passed. The area of the phase plane at the point of bifurcation is $6\pi(C^2/4A^2)^{1/3}$. Far from the resonance, where the mutual inclination is constant, this area is $\pi(p^2 + q^2) = 2\pi R = 4\pi(L' - S) \sin^2 (\epsilon/2)$. Thus, the mutual inclination after passage through the eviction resonance satisfies

$$\sin^2 \frac{\epsilon}{2} = \frac{3}{L' - S} \left(\frac{C^2}{4A^2}\right)^{1/3} . \tag{20}$$

If the initial mutual inclination of the lunar orbit is negligibly small, then the posteviction mutual inclination is approximately

$$\sin \epsilon \approx 2\sqrt{3}\left(\frac{5}{264}\right)^{1/3}\left(\frac{n_2^2}{n_1^2}\frac{a_1^2}{J_2 R_E} e^2 \sin I\right)^{1/3} \times \left(1 - \frac{7e^2}{12} + \cdots\right) . \tag{21}$$

Evaluating this expression for the run displayed in Figure 2, we find a posteviction mutual inclination of about 3°.1, which is close to that observed in the numerical experiment displayed, though a little high. We find that for slower rates of tidal evolution the predicted jump is in closer agreement with the numerical experiments, indicating that for the run displayed the passage through eviction is not sufficiently adiabatic.

Unfortunately, the eviction by itself does not solve the mutual inclination problem. At this point in the evolution, the mutual inclination must be excited to about 12° for the Earth-Moon system to evolve to its present configuration, presuming no other resonances are encountered that can further excite the mutual inclination.

10. A SECOND ENCOUNTER WITH EVICTION

If the system is captured by the evection, then the eccentricity after the encounters with the evection/eviction resonances is substantial, perhaps as large as 0.5. The eccentricity that is excited by the evection passage depends on the A-parameter (see Fig. 6). The eccentricity has its largest excitation for $A = 0$ and is reduced for larger A. The evolution after passage through the evection depends on A. If A is small, the large postevection eccentricity continues to grow larger, but if A is large then the small postevection eccentricity initially decays but later starts to grow again. Evidently, if the value of A is too small then there is no way to connect the evolution to the present lunar eccentricity.

There appear to be two possibilities. If A is initially large enough, then the evection excitation is relatively small, the postevection evolution brings the system to lower eccentricity, and connection to the present eccentricity is possible with a gradual decrease of A, perhaps through cooling in the Moon, to the observed value near 1. Unfortunately, this track does not yield the correct lunar inclination. Recall that the eviction excitation is proportional to $e^{2/3}$. If the postevection eccentricity is small, then the mutual inclination excitation at the eviction is small.

On the other hand, if the initial A is small, then the excitation of eccentricity at evection can be large, and continues to grow after evection passage. Now the Moon would be substantially hotter after its excursion along the evection/eviction route. As long as the eccentricity remains large, the Moon is subject to strong tidal heating. Investigations for Io (Peale et al. 1979) suggest that substantial tidal heating lowers the effective Q and increases A. How much is uncertain. If the effective A-parameter is moderate, the eccentricity of the Moon will continue to increase as the Moon continues to evolve outward, with continued tidal heating. Eventually, in order to connect to the present state of the system, the A-parameter must become large enough to sufficiently damp the eccentricity of the lunar orbit. How far out in semimajor axis and how high the eccentricity would become before this happens are unknown. All we can deduce is that if the Earth-Moon system was once captured by the evection, then there must have been a period of sufficiently enhanced dissipation in the Moon so that the A-parameter would be large enough to wipe away the memory of the high-eccentricity interval. It seems likely that the high-dissipation interval coincides with the evection resonance passage itself or soon thereafter.

If, as a consequence of strong tidal heating, the A-parameter is suddenly increased, then the subsequent evolution will be dramatically altered. Strong dissipation in the Moon not only damps the eccentricity of the lunar orbit but can cause the semimajor axis of the Moon to go through a period of regression. This sort of evolution was demonstrated by Mignard (1981). We can understand this by a simple argument. Tides in the Moon dissipate energy but conserve angular momentum. The orbital angular momentum involves the product $a(1 - e^2)$, so conservation of angular momentum causes a to decrease as e decreases. If the dissipation in the Moon is strong enough, this tendency of lunar tides to decrease the semimajor axis can win over the tendency of Earth tides to increase the lunar semimajor axis. The passage through the evection resonance is followed closely by the passage through the eviction resonance. If this interval of enhanced tidal dissipation occurs after the passage through eviction, then the regression of the semimajor axis can carry the system once more through the eviction resonance. However, this time the passage through the resonance is in the direction for which capture is possible. Indeed, if the eccentricity has not decayed too much, capture into the eviction is almost certain.

We have made quite a few simulations to explore this process. We have taken a typical $A = 0$ post-evection/eviction system state and evolved the system with a variety of A-parameters and rates of tidal evolution. We investigated $A = 1, 3, 5, 8$, and 10 and Earth tidal dissipation rates that, if acting alone, would result in rate of semimajor-axis evolution of $da/dt|_E = 0.1, 0.2, 0.3$, and 0.4 km yr^{-1}. We found that runs with $A > 1$ and $A\, da/dt|_E \leq 2$ km yr^{-1} are captured by the eviction. Capture in the eviction during this phase requires somewhat slower evolution than is required for capture into the evection.

The initial regression of the semimajor axis as the eccentricity decreases is illustrated in Figure 9. The evolution of the mutual inclination is shown in Figure 10. For this simulation $A = 10$ and $da/dt|_E = 0.2$ km yr^{-1}.

For those runs that are captured, the subsequent evolution is remarkably insensitive to the parameter values. In

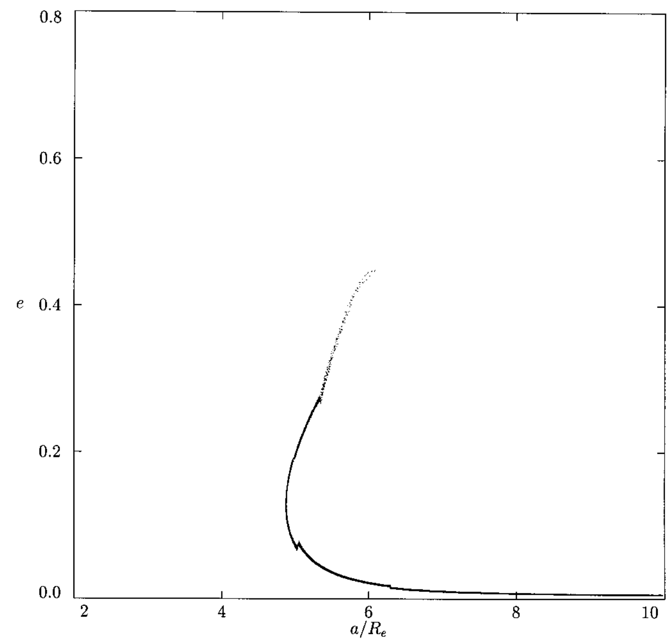

FIG. 9.—Initial regression of the semimajor axis as the eccentricity decreases, as a result of enhanced dissipation in the Moon.

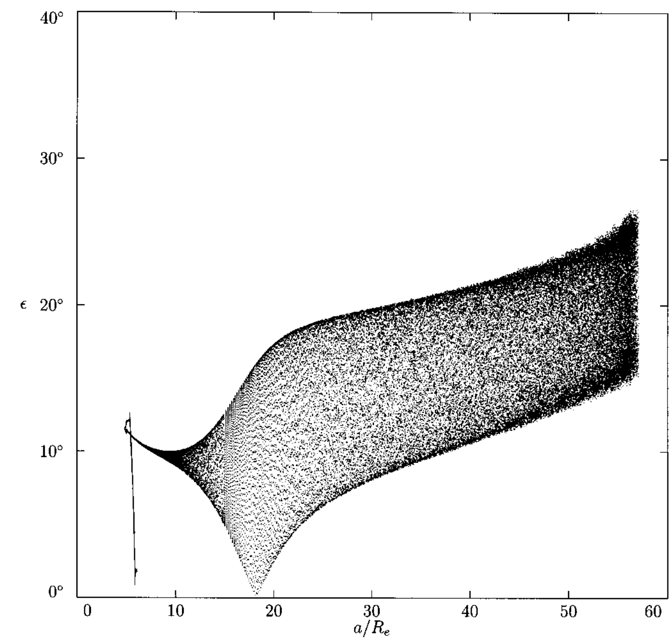

FIG. 11.—Evolution of the Earth-Moon system from an initial equatorial lunar orbit, through the evection and eviction resonances, to the present time. The result is consistent with the current inclination of the lunar orbit.

every case the mutual obliquity shoots up to values in the range 9°–13° before the system escapes.

The mechanism of escape from the eviction is simple and can be understood in terms of the eviction action, which is the area on the (p, q) eviction phase plane (see § 9). After capture, the eviction action has a value near the area of the separatrix at the point of bifurcation that forced the initial excitation in the forward passage though eviction. We observe in the simulations that the action grows as the evolution in the eviction proceeds. We also note that the allowed area in the libration region is shrinking because the strength of the eviction resonance is proportional to the square of the eccentricity, which is decreasing. So eventually the system must escape the eviction.

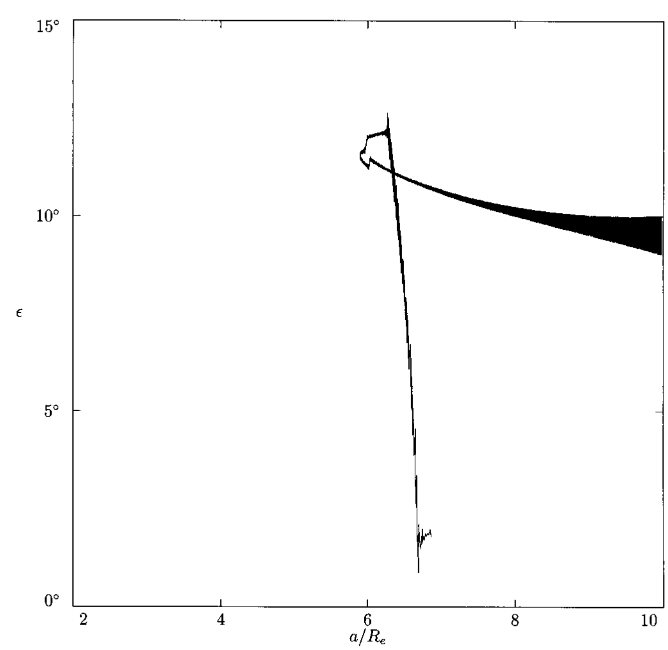

FIG. 10.—Evolution of the mutual inclination if the system is captured by the eviction during an interval of enhanced lunar dissipation. The system escapes with a mutual inclination of about 12°, just what is needed to resolve the mutual inclination problem.

After escape from the eviction, the mutual inclination is left in the range 9°–13°. The eccentricity continues to decrease because of the enhanced A. After the eccentricity declines sufficiently, the semimajor axis resumes its outward journey. The eviction resonance is passed a third time, but this time the eccentricity is small enough that there is no substantial excitation.

The eccentricity can evolve to the present eccentricity if the A-parameter is reduced to the present value (presumably by cooling) in an appropriate way.

The excitation of the mutual inclination is in just the right range so as to solve the mutual inclination problem. If we evolve the system onward from this point to the present, the current configuration of the system, including the inclination of the Moon, can be recovered. Figure 11 shows the evolution of the mutual inclination. In this simulation, the final obliquity of Earth is a couple of degrees too small. A small increase of the initial obliquity would remove this discrepancy without substantially changing the overall evolution.

11. SUMMARY

The Earth-Moon system encounters a strong orbital resonance near $a = 4.6R_{\mathrm{E}}$, a resonance between the rate of precession of the pericenter of the Moon and the mean motion of the Sun. The resonance is known as the evection resonance. The evection resonance has the same phase-space structure and bifurcations as a second-order mean motion resonance.

Capture in this resonance is certain if the rate of tidal evolution is slow enough. Evolution in the resonance can pump up the eccentricity of the Moon to values as large as 0.5, depending on the amount of dissipation in the Moon.

Escape from the evection occurs when the eccentricity reaches that value for which the tidal evolution of the semimajor axis goes to zero. The libration amplitude is unstable to further tidal evolution, and the system leaves the resonance. The evection resonance does not have a stable tidal equilibrium.

After leaving the evection resonance, the system immediately encounters a resonance that we have christened the "eviction." This is a resonance between the argument of the evection and the motion of the node of the lunar orbit on the equator of Earth. This resonance is encountered in the wrong direction for the system to be captured, but as the resonance is crossed the mutual inclination is excited by about 3°.

If indeed the Earth-Moon system was captured by the evection, then the Moon underwent significant tidal heating. There are too many uncertain parameters to precisely predict the energy input, but it is on the order of 10^{36} ergs. This is about 2 orders of magnitude larger than the total energy input from tidal heating (over the age of the solar system) as calculated by Peale & Cassen (1978). Indeed, it is comparable to the total radiogenic heating over the age of the solar system, but it is deposited in less than 10,000 years. The energy input is enough to raise the temperature of the whole Moon by 1000 K or more, presumably resulting in substantial melting. Perhaps evolution through the evection contributes to the heat required to generate the magma ocean and mare volcanism.

If the tidal heating enhances the rate of dissipation in the Moon sufficiently, then the system can encounter the eviction resonance a second time and be captured. Evolution in the eviction resonance carries the mutual inclination to the range 9°–13°, just the sort of excitation that is required to solve the mutual inclination problem. Evolution of the system from this epoch to the present can recover the current configuration of the system, including the correct inclination of the Moon.

The scenario described resolves the mutual inclination problem and provides a heat source for the lunar magma ocean. However, there are many uncertain aspects, and the connection of the changing physical properties of Earth and the Moon to the simple bulk parameters in our tidal models is tenuous. Still, we hope that this discussion will add a new dimension to studies of the origin and evolution of the Earth-Moon system. The influence of the Sun, in the form of the evection resonance, on the evolution of the protolunar disk and the accretion of the Moon deserves a closer look.

The richness of the dynamics of the Earth-Moon system is far from being exhausted. Other resonances could be encountered for other evolutionary tracks that we have not fully explored here. In particular, a Moon that is allowed to develop a large eccentricity (around 0.6) at a distance of $28R_{\rm E}$ encounters a secular inclination-eccentricity resonance that excites the mutual inclination. Also, the rotational dynamics of the Moon was essentially ignored in our study. We should investigate the assumed lunar synchronous rotation and its stability, as well as the attitude stability of the Moon and reexamine the evolution of its Cassini states in view of the newly uncovered orbital resonances. Clearly, there is much to be done.

We thank Tim Grove, Stan Peale, Sean Solomon, Dave Stevenson, Bill Ward, and Maria Zuber for many helpful discussions. This research was supported in part by NASA through the Planetary Geology and Geophysics program, in part by the Canadian Institute for Theoretical Astrophysics (CITA), and in part by a Harlan Smith Fellowship at the University of Texas.

REFERENCES

Borderies, N., & Goldreich, P. 1984, Celest. Mech., 32, 127
Boss, A. P., & Peale, S. J. 1986, in Origin of The Moon, ed. W. K. Hartmann, R. J. Phillips, & G. J. Taylor (Houston: Lunar Planet. Inst.), 59
Brouwer, D., & Clemence, G. M. 1961, Methods of Celestial Mechanics (New York: Academic)
Burns, J. A. 1986, in Satellites, ed. J. A. Burns & M. S. Matthews (Tucson: Univ. Arizona Press), 117
Cassen, P., Reynolds, R. T., Graziani, F., Summers, A., McNellis, J., & Blalock, L. 1979, Phys. Earth Planet. Inter., 19, 183
Dickey, J. O., et al. 1994, Science, 265, 482
Goldreich, P. 1963, MNRAS, 126, 256
———. 1966, Rev. Geophys., 4, 411
Henrard, J. 1982, Celest. Mech., 27, 3
Ida, S., Canup, R. M., & Stewart, G. R. 1997, Nature, 389, 353
Kaula, W. M., & Yoder, C. 1976, in Lunar Science VII (Houston: Lunar Sci. Inst.), 440
Kirk, R. L., & Stevenson, D. J. 1989, J. Geophys. Res., 94, 12133
Mignard, F. 1981, Moon Planets, 24, 189
Peale, S. J., & Cassen, P. 1978, Icarus, 36, 245
Peale, S. J., Cassen, P., & Reynolds, R. T. 1979, Science, 203, 892
Solomon, S. C., & Chaiken, J. 1976, in Proc. 7th Lunar Sci. Conf. ed. R. B. Merrill, R. V. Morris, J. M. Rhodes, & T. M. Usselman (New York: Pergamon), 3229
Solomon, S. C., & Longhi, J. 1977, in Proc. 8th Lunar Sci. Conf. (New York: Pergamon), 583
Sonett, C. P., Kvale, E. P., Zakharian, A., Chan, M. A., & Demko, T. M. 1996, Science, 273, 100
Thompson, C., & Stevenson, D. J. 1988, ApJ, 333, 452
Touma, J., & Wisdom, J. 1994, AJ, 108, 1943
Yoder, C. 1979, Celest. Mech., 19, 3
Yoder, C., & Peale, S. J. 1981, Icarus, 47, 1